ELEMENTARY PARTICLES AND FIELDS
Experiment

Cosmic Ray Study at the Astrophysical Complex TAIGA: Results and Plans

**L. A. Kuzmichev[1]*, I. I. Astapov[2], P. A. Bezyazeekov[3], M. Blank[4], E. A. Bonvech[1],
A. N. Borodin[5], M. Brueckner[6], N. M. Budnev[3], A. V. Bulan[1], D. V. Chernov[1],
A. Chiavassa[7], A. N. Dyachok[3], A. R. Gafarov[3], A. Yu. Garmash[8],[9], V. M. Grebenyuk[5],
O. A. Gress[3], T. I. Gress[3], A. A. Grinyuk[5], O. G. Grishin[3], D. Horns[4], A. L. Ivanova[9],[3],
N. N. Kalmykov[1], V. V. Kindin[2], S. N. Kiryuhin[3], R. P. Kokoulin[2], K. G. Kompaniets[2],
E. E. Korosteleva[1], V. A. Kozhin[1], E. A. Kravchenko[8],[9], A. P. Kryukov[1],
A. A. Lagutin[10], M. V. Lavrova[5], Yu. Lemeshev[3], B. K. Lubsandorzhiev[11],
N. B. Lubsandorzhiev[1], A. D. Lukanov[11], D. Lukyantsev[3], R. R. Mirgazov[3],
R. Mirzoyan[12],[1], R. D. Monkhoev[3], E. A. Osipova[1], A. L. Pakhorukov[3], A. Pan[5],
L. V. Pankov[3], A. D. Panov[1], A. A. Petrukhin[2], D. A. Podgrudkov[1], V. A. Poleschuk[3],
E. G. Popova[1], A. Porelli[6], E. B. Postnikov[1], V. V. Prosin[1], V. S. Ptuskin[13],
A. A. Pushnin[3], R. I. Raikin[10], A. Razumov[1], E. Rjabov[3], G. I. Rubtsov[11],
Y. I. Sagan[5],[14], V. S. Samoliga[3], A. Yu. Sidorenkov[11], A. A. Silaev[1], A. A. Silaev, Jr.[1],
A. V. Skurikhin[1], M. Slunecka[5], A. V. Sokolov[8],[9], Y. Suvorkin[3], L. G. Sveshnikova[1],
V. A. Tabolenko[3], A. B. Tanaev[3], B. A. Tarashansky[3], M. Ternovoy[3], L. G. Tkachev[5],[14],
M. Tluczykont[4], N. Ushakov[11], A. Vaidyanathan[8], P. A. Volchugov[1], N. V. Volkov[10],
D. Voronin[11], R. Wischnewski[6], I. I. Yashin[2], A. V. Zagorodnikov[3], and D. P. Zhurov[3]**

Abstract—TAIGA (Tunka Advanced Instrument for cosmic ray physics and Gamma Astronomy) Astrophysical complex is being developed for studies of gamma rays and charged cosmic rays in the energy range of $10^{13}-10^{18}$ eV. The complex is located in the Tunka Valley, about 50 km from Lake Baikal. In this report we present the experiment status and plans for study of high-energy cosmic-ray physics as well as main results reached by wide-angle TAIGA-HiSCORE and Tunka-133 Cherenkov arrays of the Astrophysical complex. Plans to study cosmic rays by means of other arrays of the complex, namely scintillation array Tunka-Grande and new TAIGA-muons array and system of IACT telescopes, are discussed too.

[1] Skobeltsyn Institute of Nuclear Physics Moscow State University, Moscow, 119991 Russia.

[2] National Research Nuclear University "MEPhI" (Moscow Engineering Physics Institute), Moscow, 115409 Russia.

[3] Research Institute of Applied Physics, Irkutsk State University (API ISU), Irkutsk, 664003 Russia.

[4] Institute of Experimental Physics of Hamburg University, 22761 Hamburg, Germany.

[5] Joint Institute for Nuclear Research, Dubna, Moscow oblast, 141980 Russia.

[6] Deutsches Elektronen-Synchrotron DESY, 15738 Zeuthen, Germany.

[7] Physics Department of the University of Torino and the National Institute of Nuclear Physics INFN, 10125 Torino, Italy.

[8] Novosibirsk State University, Novosibirsk, 630090 Russia.

[9] Budker Institute of Nuclear Physics of the Siberian Branch of the Russian Academy of Sciences, Novosibirsk, 630090 Russia.

[10] Altai State University, Barnaul, 656049 Russia.

[11] Institute for Nuclear Research of the Russian Academy of Sciences, Moscow, 117312 Russia.

[12] Max Planck Institute for Physics, D-80805 Munich, Germany.

[13] Pushkov Institute of Terrestrial Magnetism, Ionosphere and Radio Wave Propagation of the Russian Academy of Sciences (IZMIRAN), Troitsk, Moscow, 108840 Russia.

[14] Dubna State University, Dubna, Moscow oblast, 141982 Russia.

*E-mail: kuz@dec1.sinp.msu.ru

1. INTRODUCTION CR IN ENERGY RANGE 10^{14}–10^{18} eV

The progress in understanding the nature of sources of high-energy cosmic rays from our Galaxy and from the Metagalaxy is going along three directions:

1. The study of secondary gamma quanta, produced by cosmic rays (CR) in the vicinity of the source, where particles are accelerated.

2. High-energy neutrinos produced in hadronic interactions are studied by neutrino telescopes.

3. The precise determination of the energy spectrum, mass composition and anisotropy of CRs by detailed measurements of all EAS parameters.

Now at the Astrophysical Complex TAIGA [1, 2] we follow both first and third approaches but in this paper only results connected with the third approach will be discussed. Status of gamma-ray astronomy investigation will be presented in another paper of this proceedings.

2. INSTALLATIONS FOR STUDY OF COSMIC RAYS IN THE TUNKA VALLEY

The EAS experiments in the Tunka valley started in 1993. The site is located 50 km west of Lake Baikal, at 51.49° N, 103.04° E at 670 m a.s.l. The Tunka valley is famous for its weather conditions. It is situated between two mountain ridges, the branch of the Sayany mountains from the North and the Hamar-Daban ridge from the South, and has a very dry climate. The first array at Tunka site Tunka-4, consisted of 4 PMTs QUASAR-370 [3]. The next stage, Tunka-13, consisted of 13 PMTs of the same type and was in operation from 1996 to 1999.

At the moment, the following installations are operating as part of the complex: Tunka-133, Tunka-Grande, TAIGA-HiSCORE, TAIGA-MUON, TAIGA-IACT (Fig. 1). Settings of all installations are synchronized with each other with an accuracy of 10 ns. The synchronization method is described in detail in [4]. Below we briefly describe both current setup and one out of operation, on which cosmic rays have been studied or will be studied.

2.1. Tunka-25 (2000–2005)

In 2000, the array Tunka-13 was modified by increasing the number of detectors to 25. This array was named Tunka-25 [5] and operated until 2005. The array consisted of 25 optical detectors, arranged in a quadratic grid with a spacing of 85 m, covering an area of about 0.1 km². The optical detectors were based on the PMT QUASAR-370. This is a hybrid phototube consisting of an electro-optical preamplifier with a hemispherical photocathode of 37-cm diameter.

2.2. Tunka-133

The Tunka-133 array consists of 175 optical detectors [6, 7]. The detectors are grouped into 25 clusters of seven detectors each—six hexagonally arranged detectors and one in the center. The distance between the detectors in a cluster is 85 m. 19 of the clusters are arranged as a dense central part of the array with a radius of about 500 m. These $19 \times 7 = 133$ stations gave the array its name. The remaining clusters are installed at distances of ≈ 1 km around the central part.

Each optical detector consists of a 50-cm diameter metallic cylinder, containing a single PMT with a hemispherical photocathode of 20 cm. The PMT output pulses are sent via 95 m RG58 coaxial cable to the center of a cluster and digitized. The cluster electronics includes the cluster controller, 4 four-channel FADC boards, an adapter unit for connection to optical detectors and a special temperature controller. The 12 bit and 200 MHz sampling FADC board is based on AD9430 fast ADCs and FPGA XILINX Spartan XC3S300 microchips. Signals from at least three optical modules of one cluster in a time window of 500 ns serve as the cluster trigger. The arrival time of local trigger is latched by the cluster clock.

2.3. Tunka-Grande

The Tunka-Grande array [8] is a network of scintillation counters combined into 19 stations, each of which can be conditionally represented as 2 parts: ground and underground, the first, consisting of 12 counters with a total area of about 8 m², detects all charged particles of EAS at the array level, the second, consisting of 8 counters with a total area of about 5 m², is located under a soil layer of 1.5 m and is designed to detect the muon component of EAS. Both parts are located in close proximity to each other. The electronics of the scintillation station is built on the basis of the electronics of the Tunka-133 installation and provides the selection of events according to external and internal trigger conditions, digitalize signals, and the transfer of information to a single DAQ center.

2.4. TAIGA-HiSCORE

The deployment of the TAIGA-HiSCORE installation [9, 10] is planned for completion in the fall of 2021. The installation will consist of 120 wide-angle optical stations (currently 86) covering an area of 1.1 km² with an inter-station spacing of 106 m.

Each optical station to contain four large area PMTs with 20 or 25 cm diameter, types EMIET9352 KB and Hamamatsu R5912 or R7081. PMT has a
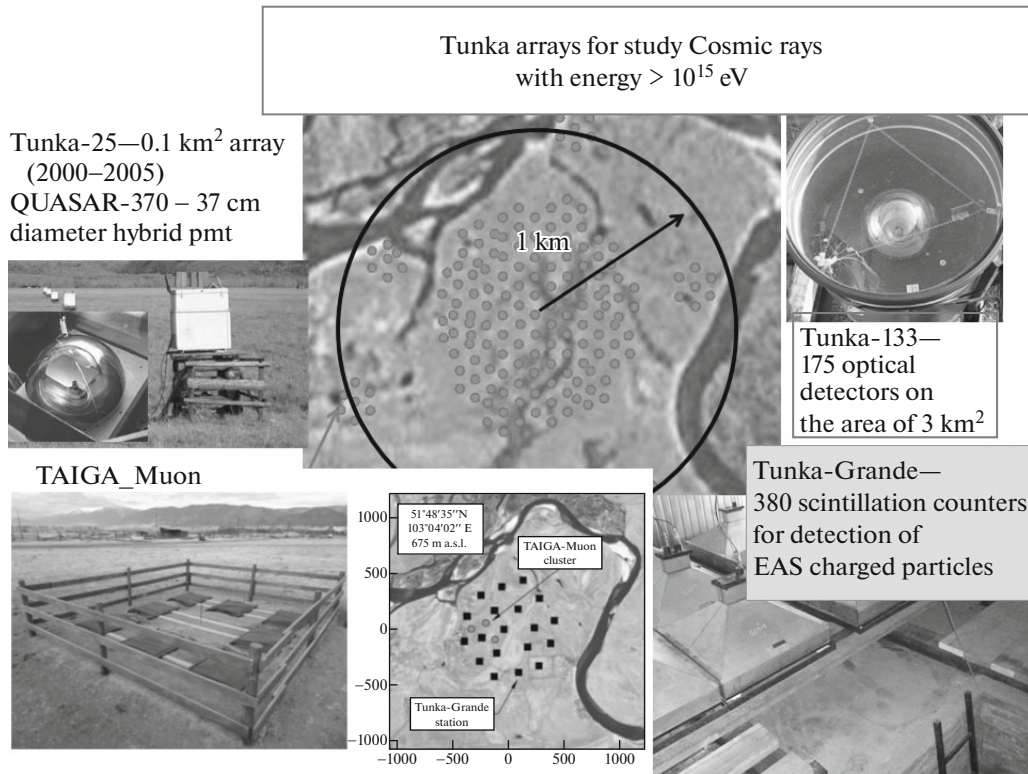
Fig. 1. Tunka arrays for study cosmic rays with energy more than 10^{15} eV.

0.4 m diameter Winston cone and a 30° viewing angle (0.6 sr).

Signals from the anode and intermediate dynode are digitized with a step of 0.5 ns by a special DRS-4 chip-based board. Stations are to be grouped in 4 clusters with independent DAQ-centers. All DAQ-centers are to be synchronized with the first one. Each station in cluster is connected with the cluster DAQ center by a fiber optic cable for data transfer and synchronization (stability ~0.2 ns)[4].

2.5. Tunka-Rex

Detection of shower radio emission is another technique that can be used to measure EAS parameters. It is mainly due to the geomagnetic deflection of relativistic electrons and positrons in the shower inducing a time-variable current. Tunka-Rex [11] is the radio array that has been running for 7 years (2012−2019) at Astrophysical complex [12]. It consisted of 63 radio antenna covering the area of 3 km². Antennas are connected to the FADC boards in the Tunka-133 clusters and in the Tunka-Grande stations. The radio data were recorded by the Tunka-133 cluster or scintillation stations local trigger.

2.6. TAIGA-MUON

The total area of muon detectors in the Tunka-Grande installation is 100 m², such an area of muon detectors is not enough to study the mass composition in the range of $10^{16}-10^{17}$ eV, which is of the greatest interest to us. We have further increased the area of muon detectors with the creation of the TAIGA-Muon array [13]. New scintillation counters covering an area of 1 m² have been developed for this installation [14]. The average signal amplitude during the passage of a muon for these counters is 20−25 photoelectrons, the inhomogeneity of the signals depending on the place of passage of the particle is ±15%, the time resolution is no less than 5 ns. It is important that these meters work when they are buried in wet soil without additional protection. In 2019, the first three clusters of the TAIGA-Muon installation were deployed, each cluster has 8 above-ground and the same number of underground meters. The counters are located in pairs, the ground ones are strictly above the underground ones. All 8 pairs are placed around the perimeter of the square with a side of 5 m. The distance between the adjacent pairs is 1 m. By 2024, it is planned to increase the area of muon meters in the TAIGA-Muon installation to 100 m².

3. METHODS OF THE EAS PARAMETERS RECONSTRUCTION

The methods of EAS parameters reconstruction were presented in several papers [8, 15]. The reconstruction of the EAS core position is performed by fitting measured amplitudes with an amplitude distance function (ADF):

$$A(R) = A(200)f(R). \qquad (1)$$

The function $f(R)$ is a fit to four different parametrizations according to the distance R (in meters) to the shower core [15]. As a measure of energy we use the Cherenkov light flux density at a core distance of 200 m—$Q(200)$. Reconstruction of $Q(200)$ is made by fitting the measured values of Qi with the lateral distribution function (LDF) [15]. The connection between the EAS energy E_0 and $Q(200)$ can be expressed by the following formula:

$$E_0 = CQ(200)^g, \qquad (2)$$

$g = 0.94$ for $10^{16}-10^{17}$ eV energy range and 0.95 for $10^{17}-10^{18}$ eV.

Constant C is found by using the results of QUEST experiment [16].

The main parameters of the EAS according to the TAIGA-HiSCORE array are reconstructed using the same algorithms and fitting functions as for the Tunka-133 installation. However, the method of determining the energy of the primary particle requires measuring the density of the light flux at a distance of 200 m from the EAS axis. For the TAIGA-HiSCORE array, this requirement is met for nearly 100% of cases only at an energy above 10^{15} eV. For lower energies, we had to develop a different algorithm. The position of the axis is determined by the center of gravity of the pulse amplitudes at no more than 5 stations. The light flux density in the center is calculated as the average value for the 2 stations closest to the axis. The calculation using the CORSIKA program showed that due to large fluctuations in the light flux density in the center, the energy measurement error is significantly greater than for 200 m, but on average, the conversion to energy is possible according to the formula:

$$\log(E_0) = C + 0.87Q_{\min}, \qquad (3)$$

$Q_{\min}$—the mean density of flux from four nearest to the core stations.

The normalization of this branch of the spectrum is carried out by comparing the densities measured by two methods in the range $10^{15}-2 \times 10^{15}$ eV.

For the Tunka-Grande array, the EAS energy is determined by the particle density at a distance of 200 m from the EAS axis [9]:

$$\log(E, \text{ eV}) = Ca \times \log(g200) + Cb. \qquad (4)$$

The coefficients Ca and Cb in this expression are determined by substituting the SHAL energy recovered from Cherenkov radiation into the left part of the equation for events recorded by both the Tunka-Grande installation and the Tunka-133 installation. The experimental dependence of E from g200 is shown in Fig. 2.

Currently, to determine X max parameter P is used, which characterizes steepness of the LDF of Cherenkov light from EAS. P is defined as the ratio of the Cherenkov light flow at a distance of 80 m from the EAS core to the flux at a distance of 200 m:

$$P = Q(80)/Q(200). \qquad (5)$$

A new MC simulation for a larger energy range confirmed that the parameter P is determined only by the thickness of the atmosphere between the array and the depth of the maximum of the EAS ($\Delta X_{\max} = 965/\cos\theta - X_{\max}, [\text{g/cm}^2]$), regardless of the energy, the zenith angle of the shower and the grade of the primary core. Here, 965 g/cm^2 is the total depth of the atmosphere at the location of the installations [17].

The calculated dependence $\Delta X_{\max}$ from P (Fig. 3) is close to linear for the range of parameter P from 2.5 to 9. The standard deviation of the points from the fitting line for this range is about 15 g/cm^2.

4. ENERGY SPECTRUM $10^{14}-10^{18}$ eV

The Tunka-133 installation [6] collected data during 7 winter seasons, in 350 clear moonless nights. The total data set time is 2175 h.

In this paper, for the TAIGA-HiSCORE installation, data obtained using 67 stations for 69 clear moonless nights in 2019−2020 are presented [18]. The total data set time is 327 h.

The energy spectrum of cosmic rays, according to the data of two installations [7, 18], is shown in Fig. 4 in comparison with the previously obtained spectrum according to the data of the Tunka-25 installation [5].

The energy spectrum smaller than 3×10^{15} eV can be described by a power law with the index $\gamma_1 = 2.70 \pm 0.01$. A form similar to the power law is observed in a sufficiently large energy range from $2 \times 10^{16} < E_0 < 3 \times 10^{17}$ eV. The power index γ_2 in this energy range is equal to 2.99 ± 0.01. Above the energy of 3×10^{17} eV (the second "knee"), the power index increases to $\gamma_3 = 3.29 \pm 0.09$. In general, it can be stated that using a single method for restoring the energy of primary particles by Cherenkov light from broad atmospheric showers, the energy spectrum of all particles in a wide range from 3×10^{14} to 3×10^{18} eV (4 orders of magnitude) was obtained.

Figure 5 shows a comparison of our data with data from other experiments. There is a good agreement,
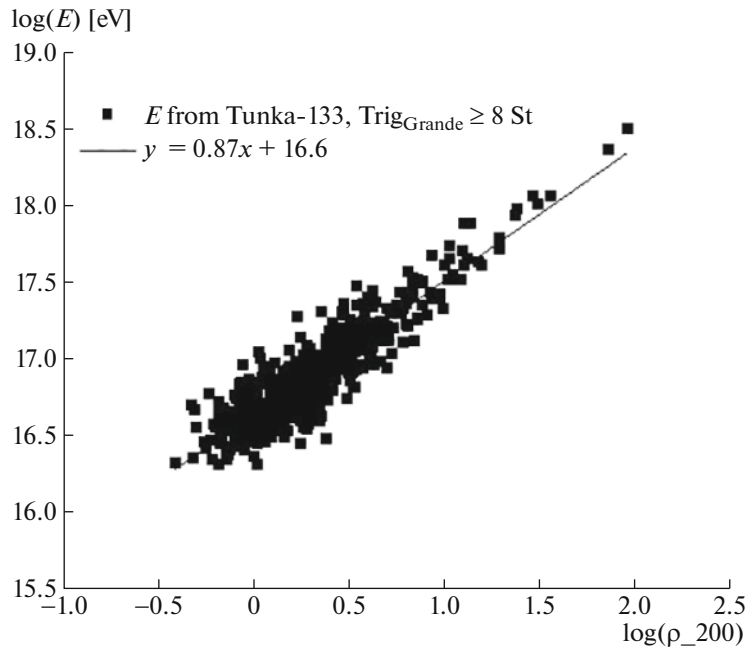
Fig. 2. The relationship between the energy of EAS and the density of charged particles at a distance of 200 m from the EAS core.
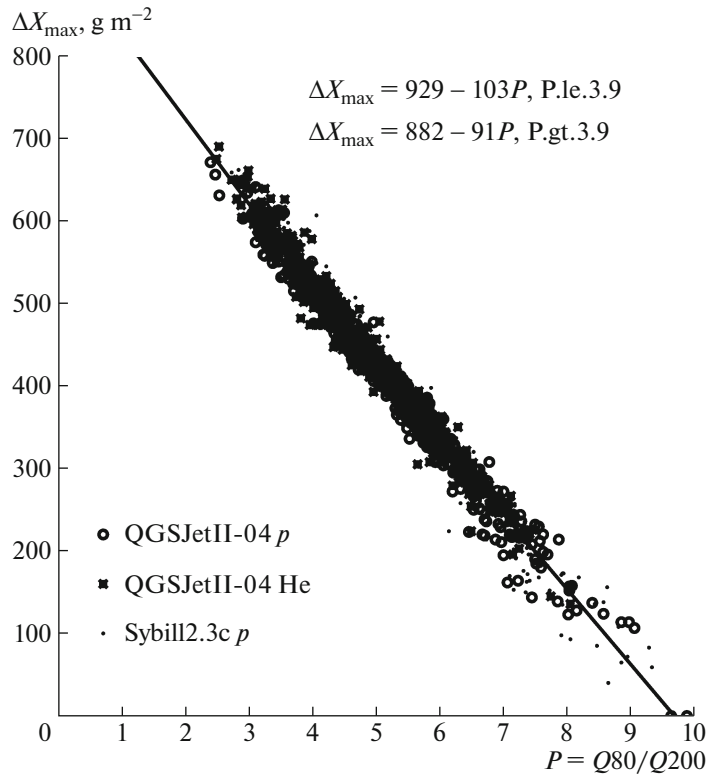
Fig. 3. Model dependence for recalculation from the steepness parameter of the FPR P to the relative position of the maximum ΔX_{max} [17].

both with direct balloon [19] and satellite [20] and high-altitude [21] measurements at low energies, and with measurements of giant installations at extremely high energies (Pierre Auger Observatory [24], Telescope Array [25]). In all experimental data, there is a decrease in the value of the spectrum index at
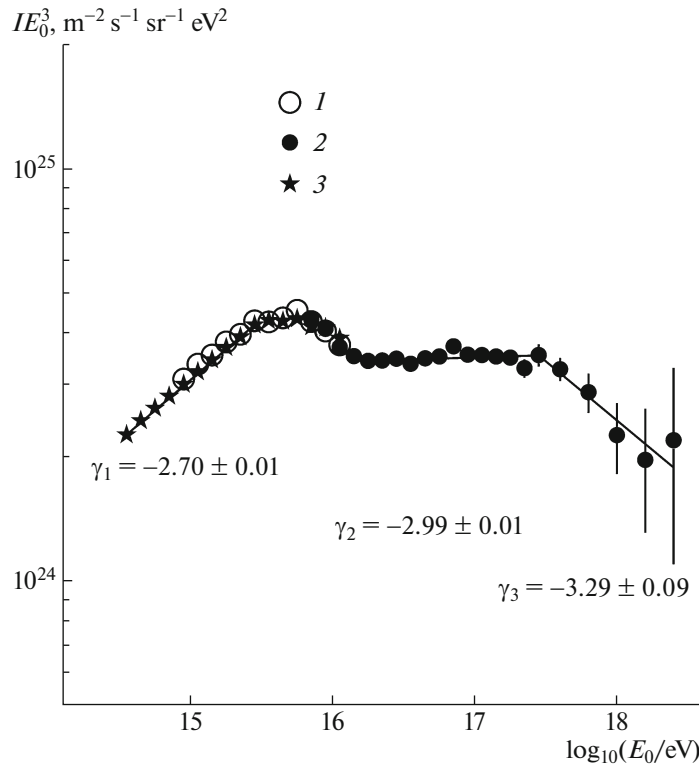
Fig. 4. The Energy spectrum of cosmic rays according to the data of the TAIGA Astrophysical complex: *1*—Tunka-25 [5], *2*—Tunka-133 [7], *3*—TAIGA-HiSCORE [18].

an energy of $(1.5-2) \times 10^{16}$ eV by an amount of $0.2-0.3$. At present, this effect has no astrophysical explanation.

5. MASS COMPOSITION $10^{15}-10^{18}$ eV

For obtaining undistorted estimates of the $X_{\max}$, EAS are selected by the zenith angle $\leqslant 30°$ and the energy at which the efficiency of the EAS detection is about 100%, for the Tunka-133 such energy is equal to 1.25×10^{16} eV, and for the TAIGA-HiSCORE—1.25×10^{15} eV.

The average depths of the maximum EAS obtained for the two installations, depending on the energy of the primary particle, are shown in Fig. 6*a*. The data of both installations, despite the difference in their geometry, fit well together, providing a wide energy range from 10^{15} to 3×10^{17} eV. Our experimental data are compared with the results of direct measurements of the maximum depth obtained by observing the fluorescent light of the EAS at PAO installations [15].

All experimental results are compared with the theoretical curves calculated using the QGSJET-II-04 model [26] for primary protons and iron nuclei.

6. PLAN FOR THE NEAREST 2–3 YEARS AND CONCLUSIONS

The development of the Astrophysical Complex in Tunka valley over 25 years has led to the construction of a number of serious installations for the study of ultrahigh-energy cosmic rays. According to the results of these installations, the energy spectrum of cosmic rays was reconstructed in the range of 4 orders of energy. A number of features are observed in the energy spectrum, which have not got an astrophysical interpretation yet First of all, the spectrum in the region of the "first knee" at an energy of $(3-6) \times 10^{15}$ eV cannot be interpreted as just a sharp change in the slope of the spectrum. The feature in the spectrum at an energy of 2×10^{16} eV, which was reliably established in a number of experiments, is to be explained in the future works as well.

Finally, the energy at which the "second knee" is located is still determined with large uncertainty. According to our data, in the range of $10^{15}-10^{17}$ eV, light nuclei—protons and helium—should dominate in the cosmic ray flux. This contradicts the break in the energy spectrum of the light component of cosmic rays predicted by the ARGOYBJ array [29], at an energy of 0.7×10^{15} eV. The dependence on the energy of mean value of $\ln A$ fits very well with the results of PAO at an energy of 3×10^{17} eV (Fig. 6*b*).
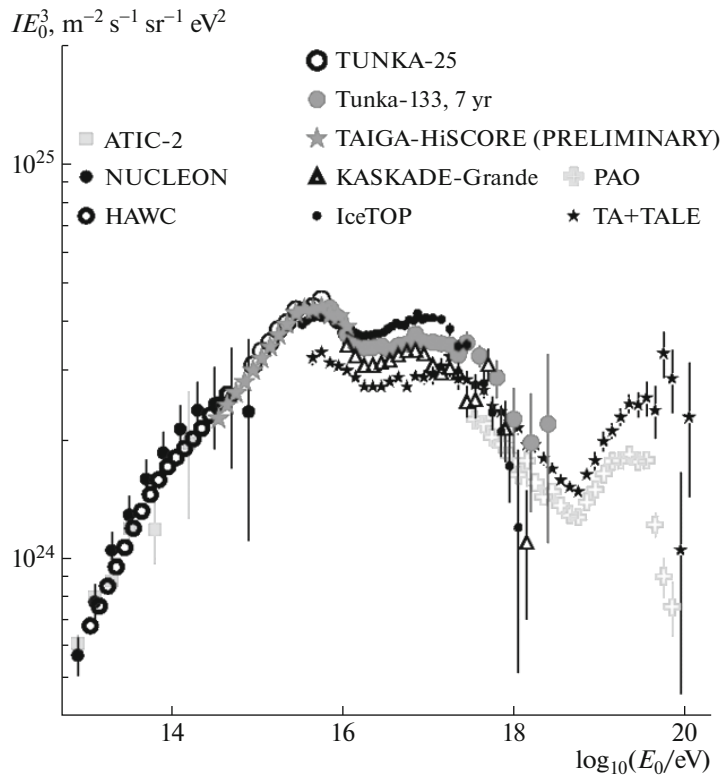
Fig. 5. Comparison of the energy spectra of cosmic rays obtained in various experiments in a wide energy range: ATIC-2 [19], NUCLEON [20], HAWC [21], Tunka-25, TAIGA-HiSCORE, Tunka-133, KASCADE-Grande [22], Ice-Top [23], PAO [24], TA + Tale [25].
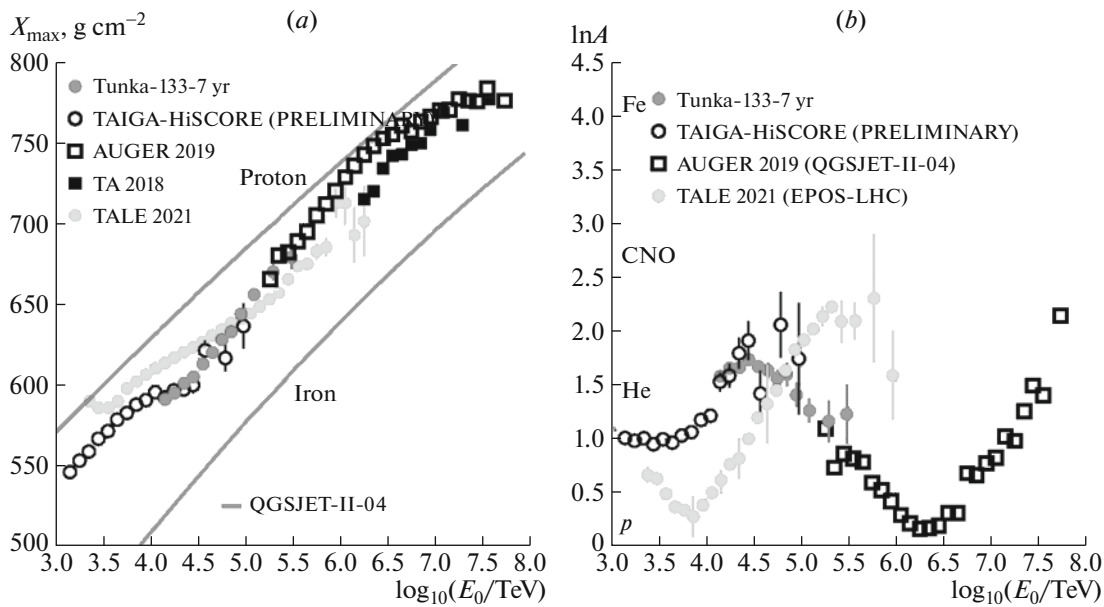
Fig. 6. (*a*) Dependence of the average depth of the mean X_{max} from the energy. (*b*) The dependence of the average logarithm of the mass $\langle \ln A \rangle$ on the energy, Dark gray circles—Tunka-133 [17], open circles—TAIGA-HiSCORE [17], open squares—PAO [27], light gray circles—TALE [28], black squares—TA [25].

It should be pointed out that according to the data on the mass composition in the area of the first knee from different experiments, it is not yet possible to get a consistent picture. Perhaps, the composition in this energy range will be finally understood only after the launch of a multi-ton detector into orbit [30].

In the next 2–3 years, the study of the mass composition, according to the available experimental

data, will be continued as one of the main topics. An attempt will be made to study the mass composition at an energy below 10^{15} eV, possibly based on joint data from the TAIGA-HiSCORE, TAIGA-IACT and small size wide-angle IACTs with SiPM-based camera [31] installations. In the range of $10^{16}-10^{17}$ eV, we hope to advance in the study of the mass composition with increase of the muon detectors area. We associate the progress in the field of energy above 10^{17} eV with the possible deployment of a new fluorescent detector as part of the Astrophysical complex TAIGA.

ACKNOWLEDGMENTS

REFERENCES

1. N. Budnev, I. Astapov, P. Bezyazeekov, A. Borodin, M. Brückner, D. Chernykh, A. Chiavassa, A. Dyachok, O. Fedorov, A. Gafarov, A. Garmash, V. Grebenyuk, O. Gress, T. Gress, A. Grinyuk, O. Grishin, et al., Nucl. Instrum. Methods Phys. Res., Sect. A **958**, 162113 (2020).

2. L. Kuzmichev, I. Astapov, P. Bezyazeekov, V. Boreyko, A. Borodin, N. Budnev, R. Wischnewski, A. Garmash, A. Gafarov, N. Gorbunov, V. Grebenyuk, O. Gress, T. Gress, A. Grinyuk, O. Grishin, A. Dyachok, et al., Phys. At. Nucl. **81**, 497 (2018).

3. R. Bagduev, V. Balkanov, I. Belolaptikov, L. Bezrukov, N. Budnev, B. Borisovets, G. Domogatsky, L. Donskych, A. Doroshenko, A. Garus, A. Golikov, B. Gluchovskoj, R. Heller, V. Kabikov, M. Khripunova, A. Klabukov, et al., Nucl. Instrum. Methods Phys. Res., Sect. A **420**, 138 (1999).

4. O. Gress, I. Astapov, N. Budnev, P. Bezyazeekov, A. Bogdanov, V. Boreyko, M. Brückner, A. Chiavassa, O. Chvalaev, A. Dyachok, N. Gress, S. Epimakhov, E. Fedoseev, A. Gafarov, N. Gorbunov, V. Grebenyuk, et al., Nucl. Instrum. Methods Phys. Res., Sect. A **845**, 367 (2017).

5. N. Budnev, D. Chernov, O. Gress, E. Korosteleva, L. Kuzmichev, B. Lubsandorzhiev, G. Navarra, L. Pankov, V. Prosin, Y. Semeney, C. Spiering, R. Wischnewski, and I. Yashin, Astropart. Phys. **50–52**, 18 (2013).

6. S. Berezhnev, S. Epimakhov, N. Karpov, N. Kalmykov, E. Korosteleva, V. Kozhin, L. Kuzmichev, B. Lubsandorzhiev, N. Lubsandorzhiev, M. Panasyuk, E. Popova, V. Prosin, V. Ptuskin, B. Shaibonov, A. Silaev, A. Silaev, Jr., et al., Nucl. Instrum. Methods Phys. Res., Sect. A **692**, 98 (2012).

7. N. Budnev, A. Chiavassa, O. Gress, T. Gress, A. Dyachok, N. Karpov, N. Kalmykov, E. Korosteleva, V. Kozhin, L. Kuzmichev, B. Lubsandorzhiev, N. Lubsandorzhiev, R. Mirgazov, E. Osipova, M. Panasyuk, L. Pankov, et al., Astropart. Phys. **117**, 102406 (2020).

8. R. Monkhoev, N. Budnev, D. Voronin, A. Gafarov, O. Gress, T. Gress, A. Dyachok, A. Zagorodnikov, V. Zurbanov, N. Kalmykov, Yu. Kazarina, S. Kiryuhin, E. Korosteleva, V. Kozhin, L. Kuzmichev, B. Lubsandorzhiev, et al., Bull. Russ. Acad. Sci.: Phys. **83**, 959 (2019).

9. M. Tluczykont, D. Hampf, D. Horns, D. Spitschan, L. Kuzmichev, V. Prosin, C. Spiering, R. Wischnewski, Astropart. Phys. **56**, 42 (2014).

10. I. Astapov, N. Barbashina, A. Bogdanov, V. Boreyko, N. Budnev, R. Wischnewski, R. Gafarov, V. Grebenyuk, O. Gress, T. Gress, A. Grinyuk, O. Grishin, N. Gorbunov, A. Dyachok, S. Epimakhov, A. Zagorodnikov, et al., Bull. Russ. Acad. Sci.: Phys. **81**, 460 (2017).

11. P. Bezyazeekov, N. Budnev, O. Gress, A. Haungs, R. Hiller, T. Huege, Y. Kazarina, M. Kleifges, E. Konstantinov, E. Korosteleva, D. Kostunin, O. Krжmer, E. Levinson, N. Lubsandorzhiev, R. Mirgazov, R. Monkhoev, et al., Nucl. Instrum. Methods Phys. Res., Sect. A **802**, 89 (2015).

12. D. Kostunin, P. Bezyazeekov, N. Budnev, O. Fedorov, O. Gress, O. Grishin, A. Haungs, T. Huege, Y. Kazarina, M. Kleifges, E. Korosteleva, L. Kuzmichev, V. Lenok, N. Lubsandorzhiev, S. Malakhov, T. Marshalkina, et al., PoS(ICRC2019) 319; arXiv: 1908.1035.

13. A. Ivanova, N. Budnev, A. Chiavassa, A. Dyachok, O. Fedorov, A. Gafarov, A. Garmash, V. Grebenyuk, O. Gress T. Gress, E. Korosteleva, L. Kuzmichev, V. Lenok, N. Lubsandorzhiev, S. Malakhov, T. Marshalkina, et al., J. Instrum. **15**, C06057 (2020).

14. I. Astapov, P. Bezyazeekov, A. Borodin, M. Brueckner, N. Budnev, A. Chiavassa, A. Dyachok, O. Fedorov, A. Gafarov, A. Garmash, N. Gorbunov, V. Grebenyuk, O. Gress, T. Gress, O. Grishin, A. Grinyuk, et al., Nucl. Instrum. Methods Phys. Res., Sect. A **936**, 254 (2019)

15. V. Prosin, S. Berezhnev, N. Budnev, A. Chiavassa, O. Chvalaev, O. Gress, A. Dyachok, S. Epimakhov, N. Karpov, N. Kalmykov, E. Konstantinov, A. Korobchenko, E. Korosteleva, V. Kozhin, L. Kuzmichev, B. Lubsandorzhiev, et al., Nucl. Instrum. Methods Phys. Res., Sect. A **756**, 94 (2014).

16. E. Korosteleva, V. Prosin, L. Kuzmichev, and G. Navarra, Nucl. Phys. B Proc. Suppl. **165**, 74 (2007).

17. V. Prosin, I. Astapov, P. Bezyazeekov, A. Borodin, M. Brückner, N. Budnev, A. Bulan, A. Vaidyanathan, R. Wischnewski, P. Volchugov, D. Voronin, A. Gafarov, A. Garmash, V. Grebenyuk, O. Gress, T. Gress, et al., Bull. Russ. Acad. Sci.: Phys. **85**, 395 (2021)

18. V. Prosin, I. Astapov, P. Bezyazeekov, V. Boreyko, A. Borodin, M. Brückner, N. Budnev, R. Wischnewski, A. Garmash, A. Gafarov, N. Gorbunov, V. Grebenyuk, O. Gress, T. Gress, A. Grinyuk, O. Grishin, et al., Bull. Russ. Acad. Sci.: Phys. **83**, 1016 (2019).

19. A. Panov, J. Adams, Jr., H. Ahn, G. Bashinzhagyan, J. Watts, J. Wefel, J. Wu, O. Ganel, T. Guzik, V. Zatsepin, I. Isbertd, K. Kim, M. Christl, E. Kouznetsov, M. Panasyuk, E. Seo, et al., Bull. Russ. Acad. Sci.: Phys. **73**, 564 (2009).

20. A. Turundaevskiy, O. Vasiliev, D. Karmanov, I. Kovalev, I. Kudryashov, F. Kurganov, A. Panov, and D. Podorozhny, Bull. Russ. Acad. Sci.: Phys. **85**, 353 (2021).

21. R. Alfaro, C. Alvarez, C. Alvarez, R. Arceo, J. Arteaga-Velazquez, D. Avila Rojas, H. A. Ayala Solares, A. S. Barber, A. Becerril, E. Belmont-Moreno, S. Y. BenZvi, C. Brisbois, K. S. Caballero-Mora, T. Capistran, A. Carraminana, S. Casanova, M. Castillo, et al., Phys. Rev. D **96**, 122001 (2017).

22. W. D. Apel, J. C. Arteaga-Velázquez, K. Bekk, M. Bertaina, J. Blümer, H. Bozdog, I. M. Brancus, P. Buchholz, E. Cantoni, A. Chiavassa, F. Cossavella, K. Daumiller, V. de Souza, F. Di Pierro, P. Doll, R. Engel, et al., Astropart. Phys. **36**, 183 (2012).

23. M. G. Aartsen, R. Abbasi, Y. Abdou, M. Ackermann, J. Adams, A. Aguilar, M. Ahlers, D. Altmann, J. Auffenberg, X. Bai, M. Baker, S. W. Barwick, V. Baum, R. Bay, J. Beatty, S. Bechet, et al., Phys. Rev. D **88**, 042004 (2013).

24. J. Abraham, P. Abreu, M. Aglietta, E. J. Ahn, D. Allard, I. Allekotte, J. Allen, J. Alvarez-Muniz, M. Ambrosio, L. Anchordoqui, S. Andringa, T. Antici, A. Anzalone, C. Aramo, E. Arganda, K. Arisaka, et al., Phys. Lett. B **685**, 239 (2010).

25. R. U. Abbasi, M. Abe, T. Abu-Zayyad, M. Allen, Y. Arai, E. Barcikowski, J. W. Belz, D. Bergman, S. A. Blake, R. Cady, B. Cheon, J. Chiba, M. Chikawa, A. Di Matteo, T. Fujii, K. Fujita, et al., Astrophys. J. **858**, 76 (2018).

26. S. Ostapchenko and M. Bleicher, Phys. Rev. D **93**, 051501 (2016).

27. A. Yushkov et al. (for the Pierre Auger Collab.), in *Proceedings of the 36th International Cosmic Ray Conference ICRC, Madison, USA, 2019*; PoS (ICRC2019) 482; arXiv: 1909.09073 (2019).

28. R. U. Abbasi, M. Abe, T. Abu-Zayyad, M. Allen, Y. Arai, E. Barcikowski, J. Belz, D. R. Bergman, S. A. Blake, R. Cady, B. Cheon, J. Chiba, M. Chikawa, T. Fujii, K. Fujisue, K. Fujita, et al., Astrophys. J. **909**, 178 (2021).

29. B. Bartoli, P. Bernardini, X. J. Bi, Z. Cao, S. Catalanotti, S. Z. Chen, T. L. Chen, S. W. Cui, B. Z. Dai, A. D'Amone, Danzengluobu, I. De Mitri, B. D'Ettorre-Piazzoli, T. Di Girolamo, G. Di Sciascio, et al., Phys. Rev. D **92**, 092005 (2015).

30. D. Karmanov, A. Panov, L. Tkachev, and A. Turundaevskiy, Bull. Russ. Acad. Sci.: Phys. **83**, 637 (2019).

31. D. Chernov, I. Astapov, P. Bezyazeekov, E. Bonvech, A. Borodin, M. Brueckner, N. Budnev, D. Chernukh, A. Chiavassa, A. Dyachok, O. Fedorov, A. Gafarov, et al., J. Instrum. **15**, C09062 (2020).